

# Antibody-Functionalized Nanowires: A Tuner for the Activation of T Cells

Viraj Bhingardive,<sup>||</sup> Anna Kossover,<sup>||</sup> Muhammed Iraqi, Bishnu Khand, Guillaume Le Saux, Angel Porgador, and Mark Schwartzman\*

 Cite This: *Nano Lett.* 2021, 21, 4241–4248

 Read Online

ACCESS |

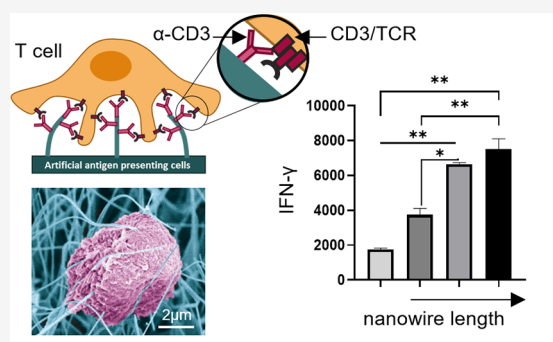
 Metrics & More

 Article Recommendations

 Supporting Information

**ABSTRACT:** T cells sense both chemical cues delivered by antigen molecules and physical cues delivered by the environmental elasticity and topography; yet, it is still largely unclear how these cues cumulatively regulate the immune activity of T cells. Here, we engineered a nanoscale platform for *ex vivo* stimulation of T cells based on antigen-functionalized nanowires. The nanowire topography and elasticity, as well as the immobilized antigens, deliver the physical and chemical cues, respectively, enabling the systematic study of the integrated effect of these cues on a T cell's immune response. We found that T cells sense both the topography and bending modulus of the nanowires and modulate their signaling, degranulation, and cytotoxicity with the variation in these physical features. Our study provides an important insight into the physical mechanism of T cell activation and paves the way to novel nanomaterials for the controlled *ex vivo* activation of T cells in immunotherapy.

**KEYWORDS:** T cells, nanowires, biofunctionalization, mechanosensing, immunotherapy



Cytotoxic T cells—the sentinels of our immune system—directly attack cancerous, infected, and stressed cells. Their immune function is regulated by activating, costimulatory, and inhibitory receptors,<sup>1,2</sup> whose binding to ligands expressed by target and antigen-presenting cells induces signaling cascades that determine the immune response. Yet, it has become progressively clear that T cells also sense physical cues of their environment, such as the spatial order of ligands<sup>3–7</sup> and elasticity,<sup>8</sup> which determine the organization and triggering of T cell receptors (TCRs).<sup>9–12</sup> Another largely unexplored physical cue is the topography of the T cell–target interface, which contains 3D nanoscale protrusions<sup>13–15</sup> with activating receptors localized at their tips.<sup>16</sup> *In vivo*, dendritic cells activate T cells with long projections (dendrites) whose geometry<sup>17</sup> and elasticity<sup>18</sup> change with the dendritic cell maturation. Still, the way mechanical and topographical cues regulate T cells' immune response is mostly unclear.

Physical regulation of T cells' response also has clinical importance. T-cell-based immunotherapy has revolutionized cancer treatment.<sup>19,20</sup> However, fast and effective *ex vivo* activation of T cells, which is a critical step in immunotherapy, remains a challenge. Currently, T cells are activated *ex vivo* using magnetic microbeads functionalized with activating antibodies. However, microbeads lack physical cues relevant to T cell activation *in vivo*, which often leads to slow expansion and compromised immune function of the resulting effector T cells. To bridge this gap, micro/nanostructures with controlled

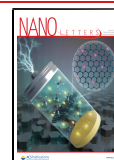
shape and elasticity are explored today as an alternative to microbeads, showing improved T cell activation due to the combined physical and chemical cues they provide.<sup>21–24</sup>

The effect of physical cues on T cell response was studied using reductionist platforms, such as arrays of elastomer micropillars.<sup>25</sup> However, *in vivo* physical cues of the T cell environment often span over the nanometer scale, and micropillars cannot mimic them. Furthermore, the micropillar stiffness spans over the MPa scale.<sup>26,27</sup> This stiffness is orders of magnitude higher than that of the T cell natural environment, which include myeloid, monocyte, and dendritic cells, whose stiffness is between hundreds to thousands of Pa,<sup>28</sup> as well as an extracellular matrix and tumor cells and tissues whose stiffnesses can reach 100 kPa.<sup>29,30</sup> Recently, we mechanically stimulated natural killer (NK) cells, cytotoxic lymphocytes of the innate immune systems, using nanowires, whose topography and compliance to the cell forces mimic those of the physiological lymphocyte environment.<sup>31</sup> We found that the nanowires functionalized with activating ligands induced enhanced activation of NK cells and thereby provided

**Received:** January 20, 2021

**Revised:** May 11, 2021

**Published:** May 14, 2021



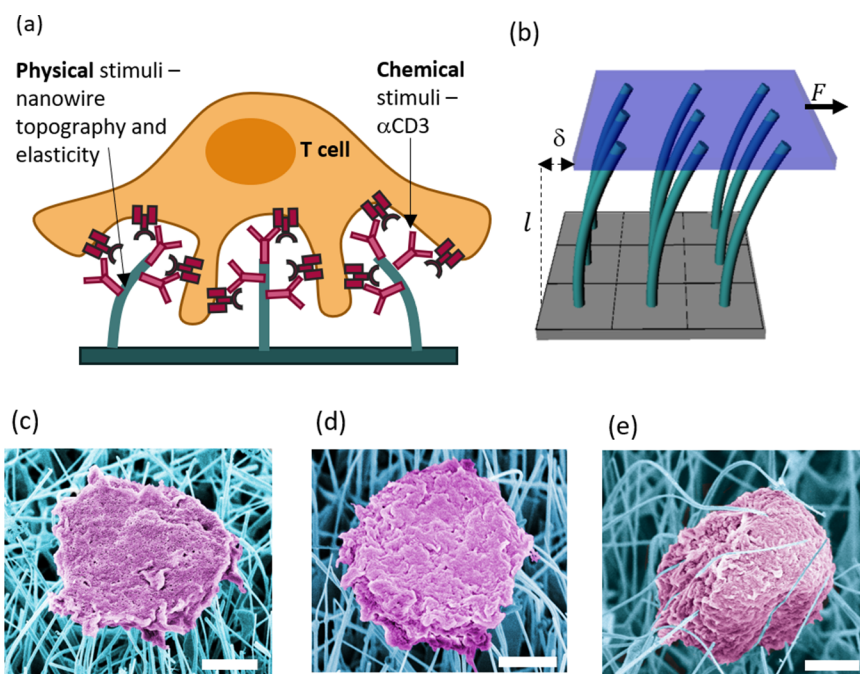


**Figure 1.** (a) Schematic illustration of the activation of T cells by ligand-functionalized nanowires. (b) Shear force applied by T cell onto nanowires, and the compliance of the nanowire forest to these forces, which is determined by the shear modulus of the nanowires. (c–e) False-colored SEM images of T cells stimulated on short, medium, and long nanowires. Scale bar = 2  $\mu\text{m}$ .

the first direct evidence that NK cells, similarly to T cells, are mechanosensitive. However, it is unclear whether the physical stimulation of NK cells by the nanowires was due to their nanotopography or due to their ultrahigh compliance to the cell forces. It is further unclear whether the sensitivity to the nanoscale physical stimuli is unique to NK cells or is generic for all lymphocytes and specifically for T cells, whose mechanosensing is a subject of intensive research.

Here, we investigated T cell sensitivity to the nanoscale topography and mechanical compliance using vertical nanowires functionalized with activating antibodies. We investigated the effect of the physical and chemical cues provided by the nanowires and antibodies, respectively, on the immune response of T cells. To discriminate between the topographical and mechanical effect of the nanowires, we used nanowires of different lengths. Such nanowires produce the same topographic environment yet different compliance to forces applied by T cells (Figure 1a,b). We found that T cells apply shear forces on the nanowires and bend them, and that the nanowire length determines T cell contraction. We further found that the signaling, degranulation, and cytotoxicity of T cells were enhanced by the nanowires and highly depended on nanowire length. However, the T cell response was greatly reduced for bare nanowires, indicating that both mechanical and chemical cues are essential for optimal T cell activation. Our findings provide an essential insight into the role of nanotopographic and nanomechanical cues in T cell response.

Vertical ZnO nanowires with an average diameter of 50 nm were grown on A-plane sapphire by chemical vapor deposition (CVD)<sup>32–34</sup> and functionalized with anti-CD3 molecules by coating the nanowires with biotin-terminated alkyl thiol, to which biotinylated anti-CD3 was then attached via a neutravidin bridge (see the SI for details). “Flat” control surfaces consisted of sapphire covered with Au nanoparticles functionalized with anti-CD3 and were used to provide similar chemical cues as functionalized nanowires, yet without the

physical cues. The functionalization was confirmed by imaging fluorescently labeled neutravidin with an epifluorescent microscope (Figure S2a,b) and with a confocal microscope (Figure S2d,e). Confocal imaging was used to quantitatively compare the functionalization on nanowires and flat surfaces. We found that the functionalization efficiency was much higher on the flat surface than that on the nanowires, probably because thiols form more robust and dense monolayers on Au than on ZnO (SI).

Primary CD8<sup>+</sup> T cells were isolated from a healthy donor (see SI) and stimulated for 3 h on nanowires grown with different lengths in the ranges of 3–5, 8–10, and 18–20  $\mu\text{m}$ , termed as short, medium, and long nanowires, respectively (Figure S1). The length was controlled by the growth time. We found that T cells contacted only the top 2–3  $\mu\text{m}$  of the nanowires, regardless of the nanowire length (Figure 1c–e). Also, the nanowires bent upon the shear forces applied by the cells. Yet, the bending strikingly depended on nanowire length—from about 1–2  $\mu\text{m}$  for short nanowires to more than 5–6  $\mu\text{m}$  for long nanowires. The nanowire bending can be described by the formula for a cantilever with a circular cross section<sup>35</sup>

$$f = \frac{3\pi E r^4}{4l^3} \delta \quad (1)$$

where  $l$  is the nanowire length,  $E$  is the Young modulus of the nanowire material, and  $r$  is the nanowire radius. For the calculation, we used an average diameter of 50 nm (Figure S1) and a Young modulus of 45 GPa based on a reported range of 30–60 GPa for ZnO nanowires.<sup>36–39</sup> Then, a 2  $\mu\text{m}$  deflection for 10  $\mu\text{m}$  nanowires implies the detection of force as small as 80 pN, which is a few orders of magnitude smaller than those that can be detected using elastomeric micropillars.<sup>40</sup> This observation highlights the potential of nanowires to detect the

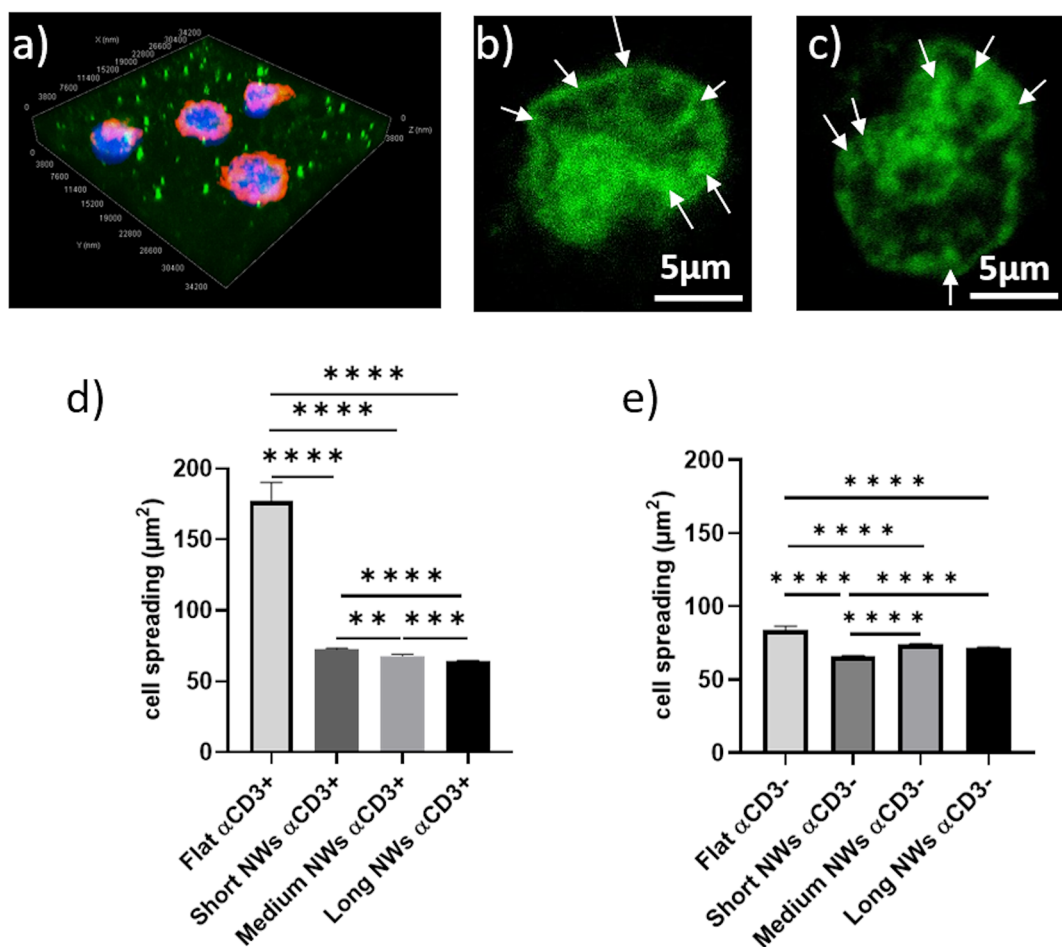


**Figure 2.** (a) Confocal 3D fluorescent image of T cells stimulated on ligand-functionalized nanowires. (b,c) Z-stack confocal microscopy image of T cells with tagged membrane onto ligand-functionalized and bare nanowires, respectively. The white arrows indicate visible invagination of the nanowires into the cell membrane. (d,e) Cell spreading onto flat surfaces and surfaces with nanowires functionalized with anti-CD3 and bare surfaces, respectively. Cell spreading was quantified by measuring the projected area of the cell cytoskeleton. The analysis was performed with Tukey's multiple-comparison tests using the GraphPad Prism software. \* $p < 0.05$ , \*\* $p < 0.01$ , \*\*\* $p < 0.001$ , \*\*\*\* $p < 0.0001$ , ns: not significant.

mechanical activity of cells, which is unattainable by existing experimental approaches.

Besides individual nanowires, the cumulative shear modulus of the nanowire forest can be assessed as a figure of merit of the environmental compliance to the cell forces. If a force  $F$  is applied on a cell area  $A$  that contacts  $N$  nanowires, the overall shear modulus can be calculated

$$\tau = \frac{F/A}{\delta/l} = \frac{Nfl}{A\delta} = \frac{N3\pi Er^4}{AA_l^2} \quad (2)$$

For an average density of three nanowires per sq. micron (Figure S1), the cumulative shear modulus ranges between 0.1 to 2.5 kPa for the nanowires of the lengths used here. This range mirrors the elasticity of myeloid, monocyte, and dendritic cells that activate T cells *in vivo*,<sup>18,28</sup> and it is hardly accessible by elastomers, which have been used so far to study T cell mechanosensing.<sup>11,12,41,42</sup> Also, the nanowire morphology has certain similarities to dendrites in dendritic cells, although it does not directly mimic the dendritic cells, which are fluidic, plastic, and chemically activates cytotoxic T cells through MHC class I molecules. Thus, the nanowires produce rather a reductionist microenvironment that stimulates T cells with controlled chemical, mechanical, and nanopopographical cues and can be used to systematically study the sensitivity of

T cells to these cues, independently and in combination with each other.

Nanowires were reported to either invaginate the cell membrane<sup>43,44</sup> or penetrate it,<sup>45–48</sup> depending on the type of cell and nanowire geometry. Here, we stained T cells incubated on the nanowires with CellMask plasma membrane stain (white) and imaged them by z-stack confocal microscopy (Figure 2a). We found that the membrane forms long projections along the nanowires, indicating that the nanowires invaginate the membrane (Figures 2b and S3). We also found that the nanowires bent toward the center of the cells, indicating that the cells applied contractile forces on the nanowires. Some of the nanowires, however, crossed each other or unevenly invaginated the membrane, probably due to the nonuniformity in the nanowire length and also due to the fact that sometimes forces applied by the cells on the nanowires deviate from the direction toward the cell center.

To elucidate the nanowire effect on the morphology of T cells, we measured their projected areas. Here, three control surfaces were used. First, a flat control surface made of sapphire with anti-CD3-functionalized Au nanoparticles provided similar chemical cues as anti-CD3-functionalized nanowires, yet without the physical cues. The second control surface contained nanowires without anti-CD3 (bare nano-

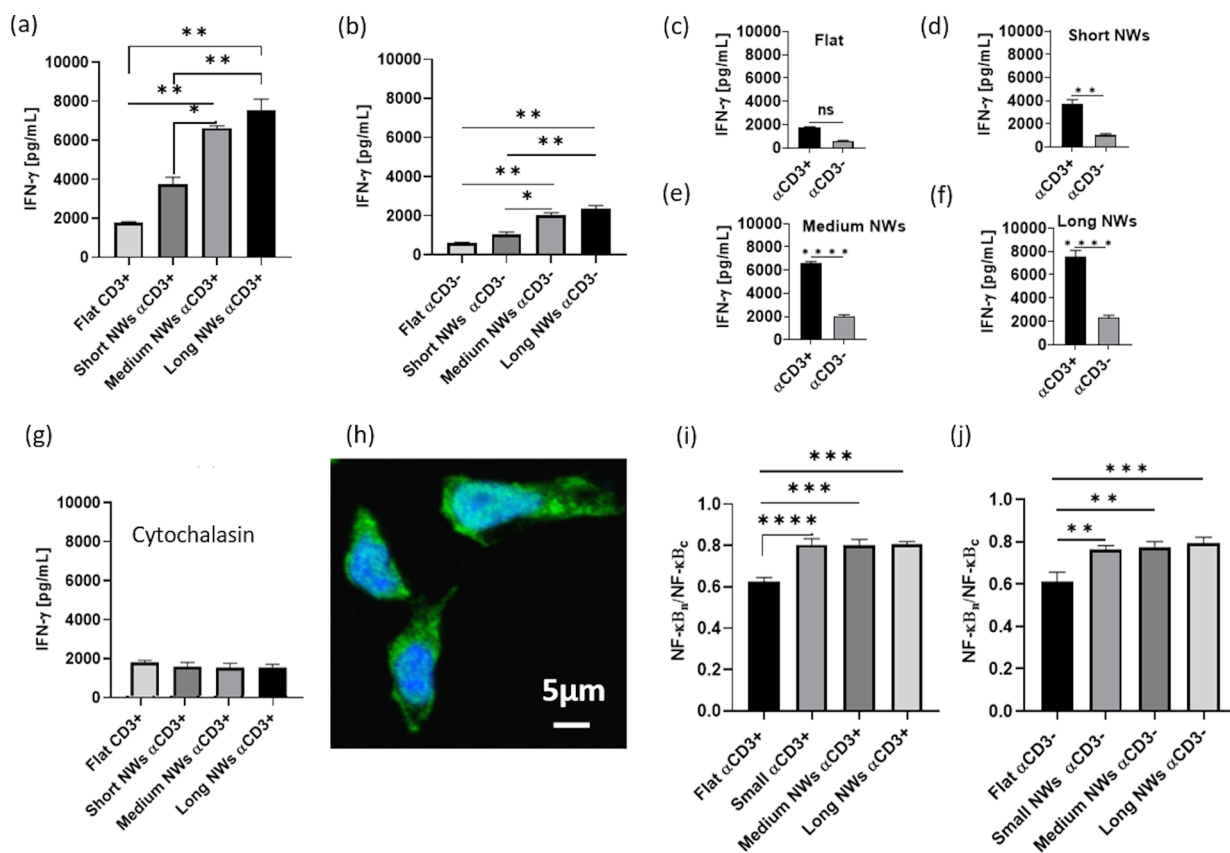


**Figure 3.** (a,b) Quantification of IFN- $\gamma$  secretion by T cells activated on flat surfaces and surfaces with nanowires with and without anti-CD3, respectively. (c–f) Effect of anti-CD3 functionalization on the activation of T cells on flat, short, medium, and long nanowire surfaces. (g) Effect of cytochalasin treatment. (h) NF- $\kappa$ B p65 staining (green) of activated T cells. (i,j) The degree of nuclear NF- $\kappa$ B translocation was determined by confocal imaging and expressed as the ratio of nuclear to cytoplasmic p65 subunits from surfaces with and without functionalization. The analysis was performed with Tukey's multiple-comparison tests using the GraphPad Prism software. \* $p < 0.05$ , \*\* $p < 0.01$ , \*\*\* $p < 0.001$ , \*\*\*\* $p < 0.0001$ , ns: not significant.

wires), and it provided the same physical cues as functionalized nanowires, yet without the chemical cues. Finally, a "bare flat" surface (sapphire covered with Au nanoparticles) lacked both the chemical and physical cues. The results are presented in Figure 2d,e. T cells on the flat functionalized surfaces had the highest projected area of about  $170 \mu\text{m}^2$ —about twice than that of functionalized nanowires. Based on the SEM images (Figure 1c–e), this relatively small area stems from the high nanowire compliance to the shear forces applied by T cells, which stimulated T cell contraction. Notably, the difference in T cell spreading between different nanowires is small, although statistically significant (Figure 2d). The fact that cell contraction increased with the nanowire further confirms that the mechanical compliance of the nanowires is at the root of the reduced T cell area on nanowires vs. that on the flat functionalized surface. Finally, it appears that anti-CD3 functionalization does not play a role in the cell morphology, as bare nanowires produced an average cell area similar to that of anti-CD3-functionalized nanowires, albeit without a clear trend or dependence on nanowire length (Figure 2e). However, the bare flat surface yielded nearly the same cell area as the nanowires did, which was also about half of that of the functionalized flat surface, probably due to the lack of anti-CD3 that promotes cell spreading.<sup>5</sup>

We next explored how the nanowire microenvironment affects T cell immune function by quantifying the secretion of interferon- $\gamma$ . To that end, we incubated T cells for 24 h and

analyzed the supernatant by ELISA. We found that functionalized nanowires, overall, induced a much higher interferon- $\gamma$  secretion than functionalized flat surfaces (Figure 3a). Furthermore, interferon- $\gamma$  secretion gradually increased with the nanowire length. On the other hand, T cells on control surfaces secreted a much lower amount of interferon- $\gamma$ , indicating the necessity of the chemical stimulus for activation (Figure 3b). Still, the level of interferon- $\gamma$  increased with the nanowire length also for bare nanowires, indicating that the physical cue alone can regulate the immune response of T cells, although the optimal stimulation requires the combination of both cues. The necessity of the chemical cue is further emphasized when directly comparing the functionalized and nonfunctionalized surfaces of each type (Figure 3c–f).

The effect of the nanowire length on T cell activation indicates that it is regulated mechanically. This regulation is a subject of extensive studies nowadays.<sup>49</sup> The immune synapse—the functional interface between T cells and antigen-presenting cells—has a highly regulated and dynamic structure, whose periphery is rich with F actin. During the synapse formation, the F actin undergoes retrograde flow due to both actin polymerization and myosin contraction, and this flow drives TCR complexes toward the synapse center.<sup>50,51</sup> The importance of actin flow and actin-generated forces was demonstrated by inhibiting actin polymerization, which affected TCR signaling and activation of T cells.<sup>52–54</sup> Here, we examined the role of actin polymerization in the nanowire-

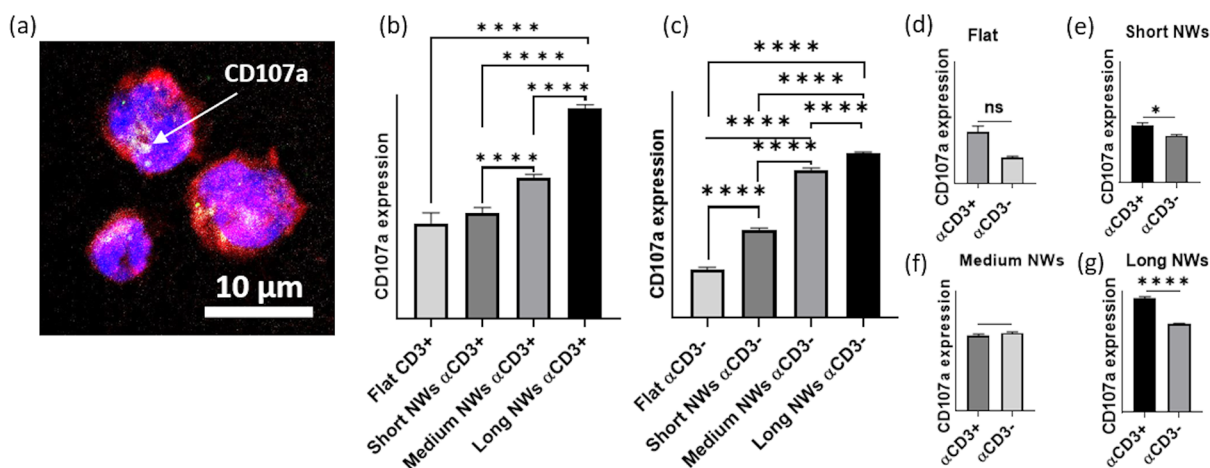


**Figure 4.** (a) Representative image of activated T cells on ligand-functionalized surfaces. Cells were stained with phalloidin for cytoskeleton (red), DAPI for nuclei (blue), and CD107a (white). (b,c) The degree of CD107a expression was quantified by measuring the fluorescence intensity of the APC-labeled anti-CD107a for surfaces with and without anti-CD3. Importantly, T cells were not permeabilized prior to the staining to avoid the detection of cytoplasmic CD107a. (d–g) Effect of anti-CD3 on activation of T cells stimulated on flat surfaces and short, medium, and long nanowires. The analysis was performed with Tukey's multiple-comparison tests using the GraphPad Prism software. \* $p < 0.05$ , \*\* $p < 0.01$ , \*\*\* $p < 0.001$ , \*\*\*\* $p < 0.0001$ , ns: not significant.

induced activation of T cells by treating them with cytochalasin that inhibits actin polymerization (Figure 3g). We found that cytochalasin barely affected the secretion of interferon- $\gamma$  on the control flat surfaces, which remained  $\sim 2000$  pg/mL, as appears in Figure 3a. However, cytochalasin reduced the interferon- $\gamma$  level of T cells on nanowires to the same level of the flat surface, regardless of the nanowire length, indicating that the inhibition of actin polymerization completely erased the nanomechanical stimulus provided by the nanowires.

We then examined how the nanowires affected T cell signaling through the nuclear translocation of NF- $\kappa$ B, which is part of the TCR signaling pathway.<sup>55</sup> To that end, we quantified p65 nuclear content by confocal microscopy of the stained p65 subunit of NF- $\kappa$ B after 18 h of incubation (Figure 3h). We found that the nanowires increased NF- $\kappa$ B translocation for both functionalized and nonfunctionalized surfaces, with a weak dependence on nanowire length (Figure 3i,j).

Finally, we assessed the effect of nanowires on the cytotoxicity of T cells through lysosome-associated membrane protein-1 (CD107a). In activated CD8+ T cells, lytic granules that contain CD107a fuse with the membrane, degranulate, and expose CD107a, making it a very commonly used marker for T cell activation.<sup>56</sup> Here, we stained T cells stimulated for 3 h with a fluorescently labeled CD107a antibody (Figure 4a). The trend of the average CD107a signal per cell closely matched that obtained for interferon- $\gamma$ : anti-CD3-functionalized nanowires, in general, induced higher CD107a than the functionalized flat surface. Also, the CD107a signal increased with nanowire length, similarly to the secretion of interferon- $\gamma$  (Figure 4c), although its absolute magnitude was lower compared to that of anti-CD3-functionalized nanowires (Figure 4d–g). This further confirms that although the nanowire-induced mechanical cues can alone stimulate T cells, their combination with the chemical cues provides optimal stimulating conditions.

Here, we produced a stimulating platform for T cells to independently assess the effects of (i) a chemical cue and (ii) two physical cues—nanotopography and elasticity on T cell activation. Our results show that the physical cues have a

striking effect on T cell response. Notably, different responses on nanowires and flat surfaces do not stem from the chemical cues: the fluorescent signal of neutravidin on the flat surface was higher than that on the nanowires (Figure S2d,e). Thus, T cells on the flat surface were exposed to a higher amount of the activating molecules. Still, the nanomechanical cues produced by the nanowires were so high that they compensated for the relatively small amount of the chemical stimulus. Even more intriguing is the comparison between differently elongated nanowires. First, SEM images of nanowires (Figure S1) confirm that all the nanowires, regardless of their length, have a similar average surface density of  $\sim 3$  nanowires per  $\mu\text{m}^2$  since. Also, SEM and z-stack confocal images of T cells on nanowires (Figures 1c–e, 2b, and S5) show that all the nanowires invaginate  $\sim 2$ – $4$   $\mu\text{m}$  of the cell membrane. We, therefore, deduce that T cells stimulated on nanowires were exposed to a similar amount of chemical and topographic cues regardless to the nanowire length. Thus, the nanowire elasticity was most probably the dominant factor in the regulation of the immune response.

It should also be noted that the chemical cue was provided here solely by anti-CD3 that triggers a CD3-TCR complex. *In vivo*, this triggering is accompanied by the triggering of costimulatory receptor CD28, whose signaling pathway is integrated with that of TCR and plays an essential role T cell response.<sup>57–59</sup> Also, CD28 triggering is used to induce T cell effector function for cancer immunotherapy.<sup>60</sup> On the other hand, T cells can also be activated solely by TCR triggering. Activation of naïve CD8+ T cells without CD28 mediated costimulation but only by a strong TCR signal—e.g., using ligands in tetramer configuration—was shown to induce effective T cell proliferation, cytokine production, and differentiation, which were unaffected by CD28 costimulation.<sup>61</sup> Reductionist platforms designed to study T cell activation commonly rely on TCR triggering alone, either by pMHC or anti-CD3,<sup>3,6,62–64</sup> to isolate the effect of TCR signaling from the signaling diversity of the natural T cell environment. Similarly, our reductionist system aims to examine the integration between mechanical and chemical cues and, for simplicity, relies only on one chemical cue that

triggers TCR. Still, the amount of this chemical cue was sufficient to achieve high activation of T cells, as CD107a and INF- $\gamma$  results indicate. In the follow-up studies, we will design more sophisticated platforms that incorporate additional costimulating or inhibitory cues and allow us to study how these cues, together with the mechanical cues provided by the nanowires, affect the response of T cells.

Our findings mirror the growing evidence of the T cell mechanosensing, which was previously observed by stimulating T cells on either elastomeric surfaces or microstructures. Interestingly, a positive trend of T cell response vs modulus was reported for the modulus range of a few hundred Pa to a few hundred kPa,<sup>42</sup> yet a negative trend was reported for the range of 0.1–2 MPa.<sup>65</sup> These studies, together, suggest that T cells might have a bell-shaped response to the variation in the environmental stiffness with a peak around 100 kPa<sup>49</sup> and that different mechanosensing mechanisms could govern T cell response at different modulus ranges. Indeed, a similar bell-shaped response to the elastomer stiffness was recently reported for NK cells.<sup>66</sup> However, flat elastomer surfaces do not mimic the nanoscale features of the T cell environment, such as membrane protrusions of antigen-presenting cells. Here, we demonstrated that these features are critical for the immune response of T cells. In contrast to the continuous elastomeric surfaces, a nanowire forest presents mechanostimulating discontinuities with multiple independent nanosized contact points at the nanowire tips, whose bending depends on the nanowire geometry. The bending moduli of individual nanowires are 440, 88, and 20 kPa for the nanowire lengths of 4, 9, and 29  $\mu\text{m}$ , respectively. These moduli are within the range for which a negative trend of activation vs modulus was reported.<sup>65</sup> The same trend was obtained here. On the other hand, the cumulative shear moduli of the nanowire forests are 2.5, 0.5, and 0.1 kPa for the nanowire lengths of 4, 9, and 29  $\mu\text{m}$ , respectively. Whether T cells sense the individual compliance of each point or their cumulative compliance is still an open question. What is clear is that the nanowire elasticity had a striking effect on T cell response. This effect was dominant over the effect of nanotopography, which was the same for all the studied nanowires. Also, cytochalasin abrogated both the activation and mechanosensitivity of the T cells, indicating a critical role of cell contractility in the cell response.

Another important factor of T cell mechanosensing is the “catch-bonds” between the TCR-CD3 complex and its ligand,<sup>67</sup> whose affinity first increases vs the applied load up to a certain peak and then decreases vs the load until the bond ruptures. This suggests that the elasticity of the substrate that supports this bond affects the receptor–ligand affinity. In our case, the elasticity depends on the nanowire length. Indeed, the cells horizontally bent nanowires by  $\sim 3 \mu\text{m}$  on average (Figure 1c–e). This required loads of 2 nN, 200 pN, and 10 pN applied on one short, medium, and long nanowire, respectively. Naturally, the mechanical loads experienced by the receptor–antibody bonds varied between differently elongated nanowires by orders of magnitude, yielding different receptor–antibody affinities and, as a result, different T cell responses.

This work provides a glimpse of how nanoscale topography, elasticity, and stimulating functionalities cumulatively regulate T cell immune response. The mechanism of regulation should be further explored, including signaling assays targeting TCR directly and its proximal signaling molecules such as LCK and

ZAP as well as downstream signaling molecules such as ERK1/2. These assays will reveal whether the nanotopography and nanofeature elasticity directly affect TCR triggering and signaling or regulate T cell response by other signaling pathways that perhaps involve cytoskeleton reorganization in the proximity of nanowires. Furthermore, the immune response of T cells leads to their apoptosis, which drastically reduces the number of activated T cells. The regulation of T cell apoptosis is important for the prevention of autoimmune processes. Future studies should be aimed at understanding whether and how the environmental nanoscale topography affects the apoptosis of T cells. Besides the fundamental mechanism of T cell activation, the nanowire platform described herein provides an intriguing perspective for the *ex vivo* T cell activation and expansion in immunotherapeutic applications. Here, the easiness and robustness with which the mechanical cues provided by the nanowires can be leveraged to produce a nanomaterial-based platform with the efficacy and control over T cell activation inaccessible to the currently used technologies.

## ■ ASSOCIATED CONTENT

### Supporting Information

The Supporting Information is available free of charge at <https://pubs.acs.org/doi/10.1021/acs.nanolett.1c00245>.

Nanowire growth process and detailed protocol about the activation of T cells (PDF)

## ■ AUTHOR INFORMATION

### Corresponding Author

Mark Schwartzman – Department of Materials Engineering and Ilse Katz Institute for Nanoscale Science and Technology, Ben-Gurion University of the Negev, Beer-Sheva 84105, Israel; [orcid.org/0000-0002-5912-525X](https://orcid.org/0000-0002-5912-525X); Phone: +972-8-6461470; Email: [marksc@bgu.ac.il](mailto:marksc@bgu.ac.il)

### Authors

Viraj Bhingardive – Department of Materials Engineering and Ilse Katz Institute for Nanoscale Science and Technology, Ben-Gurion University of the Negev, Beer-Sheva 84105, Israel

Anna Kossover – Department of Materials Engineering and Ilse Katz Institute for Nanoscale Science and Technology, Ben-Gurion University of the Negev, Beer-Sheva 84105, Israel

Muhammed Iraqi – The Shraga Segal Department of Microbiology, Immunology, and Genetics Faculty of Health Sciences, Ben-Gurion University of the Negev, Beer-Sheva 84105, Israel

Bishnu Khand – The Shraga Segal Department of Microbiology, Immunology, and Genetics Faculty of Health Sciences, Ben-Gurion University of the Negev, Beer-Sheva 84105, Israel

Guillaume Le Saux – Department of Materials Engineering and Ilse Katz Institute for Nanoscale Science and Technology, Ben-Gurion University of the Negev, Beer-Sheva 84105, Israel; [orcid.org/0000-0003-4902-1980](https://orcid.org/0000-0003-4902-1980)

Angel Porgador – The Shraga Segal Department of Microbiology, Immunology, and Genetics Faculty of Health Sciences, Ben-Gurion University of the Negev, Beer-Sheva 84105, Israel

Complete contact information is available at: <https://pubs.acs.org/doi/10.1021/acs.nanolett.1c00245>

## Author Contributions

<sup>¶</sup>V.B. and A.K. are equally contributing authors.

## Notes

The authors declare no competing financial interest.

## ACKNOWLEDGMENTS

This work was funded by the Multidisciplinary Research Grant – The Faculty of Health Science in the Ben-Gurion University of the Negev, Israel Science Foundation, Individual Grant # 1401/15, and Israel Science Foundations: F.I.R.S.T. Individual Grant # 2058/18. V.B. thanks the Negev-Tsin scholarship for its support.

## REFERENCES

- (1) *The Immune Synapse*; Baldari, C. T., Dustin, M. L., Eds.; Methods Mol. Biol.; Springer: New York, NY, 2017; Vol. 1584.
- (2) Dustin, M. L.; Groves, J. T. Receptor Signaling Clusters in the Immune Synapse. *Annu. Rev. Biophys.* **2012**, *41* (1), 543–556.
- (3) Cai, H.; Muller, J.; Depoil, D.; Mayya, V.; Sheetz, M. P.; Dustin, M. L.; Wind, S. J. Full Control of Ligand Positioning Reveals Spatial Thresholds for T Cell Receptor Triggering. *Nat. Nanotechnol.* **2018**, *13*, 610–617.
- (4) Delcassian, D.; Depoil, D.; Rudnicka, D.; Liu, M.; Davis, D. M.; Dustin, M. L.; Dunlop, I. E. Nanoscale Ligand Spacing Influences Receptor Triggering in T Cells and NK Cells. *Nano Lett.* **2013**, *13* (11), 5608–5614.
- (5) Deeg, J.; Axmann, M.; Matic, J.; Liapis, A.; Depoil, D.; Afrose, J.; Curado, S.; Dustin, M. L.; Spatz, J. P. T Cell Activation Is Determined by the Number of Presented Antigens. *Nano Lett.* **2013**, *13* (11), 5619–5626.
- (6) Matic, J.; Deeg, J.; Scheffold, A.; Goldstein, I.; Spatz, J. P. Fine Tuning and Efficient T Cell Activation with Stimulatory ACD3 Nanoarrays. *Nano Lett.* **2013**, *13* (11), 5090–5097.
- (7) Guasch, J.; Muth, C. A.; Diemer, J.; Riahinezhad, H.; Spatz, J. P. Integrin-Assisted T-Cell Activation on Nanostructured Hydrogels. *Nano Lett.* **2017**, *17* (10), 6110–6116.
- (8) Huse, M. Mechanical Forces in the Immune System. *Nat. Rev. Immunol.* **2017**, *17* (11), 679–690.
- (9) Yi, J.; Wu, X. S.; Crites, T.; Hammer, J. A. Actin Retrograde Flow and Actomyosin II Arc Contraction Drive Receptor Cluster Dynamics at the Immunological Synapse in Jurkat T Cells. *Mol. Biol. Cell* **2012**, *23* (5), 834–852.
- (10) Comrie, W. A.; Babich, A.; Burkhardt, J. K. F-Actin Flow Drives Affinity Maturation and Spatial Organization of LFA-1 at the Immunological Synapse. *J. Cell Biol.* **2015**, *208* (4), 475–491.
- (11) Judokusumo, E.; Tabdanov, E.; Kumari, S.; Dustin, M. L.; Kam, L. C. Mechanosensing in T Lymphocyte Activation. *Biophys. J.* **2012**, *102* (2), L5–L7.
- (12) O'Connor, R. S.; Hao, X.; Shen, K.; Bashour, K.; Akimova, T.; Hancock, W. W.; Kam, L. C.; Milone, M. C. Substrate Rigidity Regulates Human T Cell Activation and Proliferation. *J. Immunol.* **2012**, *189* (3), 1330–1339.
- (13) Biggs, M. J. P.; Milone, M. C.; Santos, L. C.; Gondarenko, A.; Wind, S. J. High-Resolution Imaging of the Immunological Synapse and T-Cell Receptor Microclustering through Microfabricated Substrates. *J. R. Soc., Interface* **2011**, *8* (63), 1462–1471.
- (14) Sage, P. T.; Varghese, L. M.; Martinelli, R.; Sciuto, T. E.; Kamei, M.; Dvorak, A. M.; Springer, T. A.; Sharpe, A. H.; Carman, C. V. Antigen Recognition Is Facilitated by Invadosome-like Protrusions Formed by Memory/Effector T Cells. *J. Immunol.* **2012**, *188* (8), 3686–3699.
- (15) Cai, E.; Marchuk, K.; Beemiller, P.; Beppler, C.; Rubashkin, M. G.; Weaver, V. M.; Gérard, A.; Liu, T. L.; Chen, B. C.; Betzig, E.; Bartumeus, F.; Krummel, M. F. Visualizing Dynamic Microvillar Search and Stabilization during Ligand Detection by T Cells. *Science* **2017**, *356* (6338), eaal3118.

(16) Jung, Y.; Riven, I.; Feigelson, S. W.; Kartvelishvili, E.; Tohya, K.; Miyasaka, M.; Alon, R.; Haran, G. Three-Dimensional Localization of T-Cell Receptors in Relation to Microvilli Using a Combination of Superresolution Microscopies. *Proc. Natl. Acad. Sci. U. S. A.* **2016**, *113* (40), E5916–E5924.

(17) Borg, C.; Jalil, A.; Laderach, D.; Maruyama, K.; Wakasugi, H.; Charrier, S.; Ryffel, B.; Cambi, A.; Figdor, C.; Vainchenker, W.; Galy, A.; Caignard, A.; Zitvogel, L. NK Cell Activation by Dendritic Cells (DCs) Requires The Formation of a Synapse Leading to IL-12 Polarization in DCs. *Blood* **2004**, *104* (10), 3267–3276.

(18) Blumenthal, D.; Chandra, V.; Avery, L.; Burkhardt, J. K. Mouse t Cell Priming Is Enhanced by Maturation-Dependent Stiffening of the Dendritic Cell Cortex. *eLife* **2020**, *9*, e55995.

(19) Rosenberg, S. A.; Restifo, N. P. Adoptive Cell Transfer as Personalized Immunotherapy for Human Cancer. *Science* **2015**, *348* (6230), 62–68.

(20) June, C. H.; Riddell, S. R.; Schumacher, T. N. Adoptive Cellular Therapy: A Race to the Finish Line. *Sci. Transl. Med.* **2015**, *7* (280), 280ps7.

(21) Lambert, L. H.; Goebrecht, G. K. E.; De Leo, S. E.; O'Connor, R. S.; Nunez-Cruz, S.; Li, T.; Yuan, J.; Milone, M. C.; Kam, L. C. Improving T Cell Expansion with a Soft Touch. *Nano Lett.* **2017**, *17* (2), 821–826.

(22) Dang, A. P.; De Leo, S.; Bogdanowicz, D. R.; Yuan, D. J.; Fernandes, S. M.; Brown, J. R.; Lu, H. H.; Kam, L. C. Enhanced Activation and Expansion of T Cells Using Mechanically Soft Elastomer Fibers. *Adv. Biosyst.* **2018**, *2* (2), 1700167.

(23) Fadel, T. R.; Sharp, F. A.; Vudattu, N.; Ragheb, R.; Garyu, J.; Kim, D.; Hong, E.; Li, N.; Haller, G. L.; Pfeiffer, L. D.; Justesen, S.; Herold, K. C.; Fahmy, T. M. A Carbon Nanotube-Polymer Composite for T-Cell Therapy. *Nat. Nanotechnol.* **2014**, *9* (8), 639–647.

(24) Cheung, A. S.; Zhang, D. K. Y.; Koshy, S. T.; Mooney, D. J. Scaffolds That Mimic Antigen-Presenting Cells Enable Ex Vivo Expansion of Primary T Cells. *Nat. Biotechnol.* **2018**, *36* (2), 160–169.

(25) Jin, W.; Tamzalit, F.; Chaudhuri, P. K.; Black, C. T.; Huse, M.; Kam, L. C. T Cell Activation and Immune Synapse Organization Respond to the Microscale Mechanics of Structured Surfaces. *Proc. Natl. Acad. Sci. U. S. A.* **2019**, *116* (40), 19835–19840.

(26) Saez, A.; Ghibaud, M.; Buguin, A.; Silberzan, P.; Ladoux, B. Rigidity-Driven Growth and Migration of Epithelial Cells on Microstructured Anisotropic Substrates. *Proc. Natl. Acad. Sci. U. S. A.* **2007**, *104* (20), 8281–8286.

(27) Tan, J. L.; Tien, J.; Pirone, D. M.; Gray, D. S.; Bhadriraju, K.; Chen, C. S. Cells Lying on a Bed of Microneedles: An Approach to Isolate Mechanical Force. *Proc. Natl. Acad. Sci. U. S. A.* **2003**, *100* (4), 1484–1489.

(28) Bufi, N.; Saitakis, M.; Dogniaux, S.; Buschinger, O.; Bohineust, A.; Richert, A.; Maurin, M.; Hivroz, C.; Asnacios, A. Human Primary Immune Cells Exhibit Distinct Mechanical Properties That Are Modified by Inflammation. *Biophys. J.* **2015**, *108*, 2181.

(29) Paszek, M. J.; Zahir, N.; Johnson, K. R.; Lakins, J. N.; Rozenberg, G. I.; Gefen, A.; Reinhart-King, C. A.; Margulies, S. S.; Dembo, M.; Boettiger, D.; Hammer, D. A.; Weaver, V. M. Tensional Homeostasis and the Malignant Phenotype. *Cancer Cell* **2005**, *8* (3), 241–254.

(30) Kawano, S.; Kojima, M.; Higuchi, Y.; Sugimoto, M.; Ikeda, K.; Sakuyama, N.; Takahashi, S.; Hayashi, R.; Ochiai, A.; Saito, N. Assessment of Elasticity of Colorectal Cancer Tissue, Clinical Utility, Pathological and Phenotypical Relevance. *Cancer Sci.* **2015**, *106* (9), 1232–1239.

(31) Le Saux, G.; Bar-Hanin, N.; Edri, A.; Hadad, U.; Porgador, A.; Schwartzman, M. Nanoscale Mechanosensing of Natural Killer Cells Is Revealed by Antigen-Functionalized Nanowires. *Adv. Mater.* **2019**, *31* (4), 1805954.

(32) Park, W. Il; Zheng, G.; Jiang, X.; Tian, B.; Lieber, C. M. Controlled Synthesis of Millimeter-Long Silicon Nanowires with Uniform Electronic Properties. *Nano Lett.* **2008**, *8* (9), 3004–3009.

- (33) Xie, P.; Hu, Y.; Fang, Y.; Huang, J.; Lieber, C. M. Diameter-Dependent Dopant Location in Silicon and Germanium Nanowires. *Proc. Natl. Acad. Sci. U. S. A.* **2009**, *106* (36), 15254–15258.
- (34) Cui, Y.; Lauhon, L. J.; Gudiksen, M. S.; Wang, J.; Lieber, C. M. Diameter-Controlled Synthesis of Single-Crystal Silicon Nanowires. *Appl. Phys. Lett.* **2001**, *78* (15), 2214–2216.
- (35) Landau, L. D.; Lifshitz, E. M. *Theory of Elasticity*, 3rd ed.; Pergamon Press: New York, NY, 1986; Vol. 7.
- (36) Huang, Y.; Bai, X.; Zhang, Y. In Situ Mechanical Properties of Individual ZnO Nanowires and the Mass Measurement of Nanoparticles. *J. Phys.: Condens. Matter* **2006**, *18* (15), L179.
- (37) Bai, X. D.; Gao, P. X.; Wang, Z. L.; Wang, E. G. Dual-Mode Mechanical Resonance of Individual ZnO Nanobelts. *Appl. Phys. Lett.* **2003**, *82* (26), 4806–4808.
- (38) Ni, H.; Li, X. Young's Modulus of ZnO Nanobelts Measured Using Atomic Force Microscopy and Nanoindentation Techniques. *Nanotechnology* **2006**, *17* (14), 3591–3597.
- (39) Song, J.; Wang, X.; Riedo, E.; Wang, Z. L. Elastic Property of Vertically Aligned Nanowires. *Nano Lett.* **2005**, *5* (10), 1954–1958.
- (40) Bashour, K. T.; Gondarenko, A.; Chen, H.; Shen, K.; Liu, X.; Huse, M.; Hone, J. C.; Kam, L. C. CD28 and CD3 Have Complementary Roles in T-Cell Traction Forces. *Proc. Natl. Acad. Sci. U. S. A.* **2014**, *111* (6), 2241–2246.
- (41) Zeng, Y.; Yi, J.; Wan, Z.; Liu, K.; Song, P.; Chau, A.; Wang, F.; Chang, Z.; Han, W.; Zheng, W.; Chen, Y. H.; Xiong, C.; Liu, W. Substrate Stiffness Regulates B-Cell Activation, Proliferation, Class Switch, and T-Cell-Independent Antibody Responses in Vivo. *Eur. J. Immunol.* **2015**, *45*, 1621.
- (42) Saitakis, M.; Dogniaux, S.; Goudot, C.; Bui, N.; Asnacios, S.; Maurin, M.; Randriamampita, C.; Asnacios, A.; Hivroz, C. Different TCR-Induced T Lymphocyte Responses Are Potentiated by Stiffness with Variable Sensitivity. *eLife* **2017**, *6*, e23190.
- (43) Hanson, L.; Lin, Z. C.; Xie, C.; Cui, Y.; Cui, B. Characterization of the Cell-Nanopillar Interface by Transmission Electron Microscopy. *Nano Lett.* **2012**, *12* (11), 5815–5820.
- (44) Berthing, T.; Bonde, S.; Rostgaard, K. R.; Madsen, M. H.; Sorensen, C. B.; Nygård, J.; Martinez, K. L. Cell Membrane Conformation at Vertical Nanowire Array Interface Revealed by Fluorescence Imaging. *Nanotechnology* **2012**, *23* (41), 415102.
- (45) Shalek, A. K.; Gaublonne, J. T.; Wang, L.; Yosef, N.; Chevrier, N.; Andersen, M. S.; Robinson, J. T.; Pochet, N.; Neuberg, D.; Gertner, R. S.; Amit, I.; Brown, J. R.; Hacohen, N.; Regev, A.; Wu, C. J.; Park, H. Nanowire-Mediated Delivery Enables Functional Interrogation of Primary Immune Cells: Application to the Analysis of Chronic Lymphocytic Leukemia. *Nano Lett.* **2012**, *12* (12), 6498–6504.
- (46) Na, Y. R.; Kim, S. Y.; Gaublonne, J. T.; Shalek, A. K.; Jorgolli, M.; Park, H.; Yang, E. G. Probing Enzymatic Activity inside Living Cells Using a Nanowire-Cell “Sandwich” Assay. *Nano Lett.* **2013**, *13* (1), 153–158.
- (47) Yosef, N.; Shalek, A. K.; Gaublonne, J. T.; Jin, H.; Lee, Y.; Awasthi, A.; Wu, C.; Karwacz, K.; Xiao, S.; Jorgolli, M.; Gennert, D.; Satija, R.; Shakya, A.; Lu, D. Y.; Trombetta, J. J.; Pillai, M. R.; Ratcliffe, P. J.; Coleman, M. L.; Bix, M.; et al. Dynamic Regulatory Network Controlling TH17 Cell Differentiation. *Nature* **2013**, *496* (7446), 461–468.
- (48) Prinz, C. N. Interactions between Semiconductor Nanowires and Living Cells. *J. Phys.: Condens. Matter* **2015**, *27* (23), 233103.
- (49) Basu, R.; Huse, M. Mechanical Communication at the Immunological Synapse. *Trends Cell Biol.* **2017**, *27* (4), 241–254.
- (50) Hammer, J. A.; Burkhardt, J. K. Controversy and Consensus Regarding Myosin II Function at the Immunological Synapse. *Curr. Opin. Immunol.* **2013**, *25* (3), 300–306.
- (51) Le Floch, A.; Huse, M. Molecular Mechanisms and Functional Implications of Polarized Actin Remodeling at the T Cell Immunological Synapse. *Cell. Mol. Life Sci.* **2015**, *72* (3), 537–556.
- (52) Campi, G.; Varma, R.; Dustin, M. L. Actin and Agonist MHC-Peptide Complex-Dependent T Cell Receptor Microclusters as Scaffolds for Signaling. *J. Exp. Med.* **2005**, *202* (8), 1031.
- (53) Barda-Saad, M.; Braiman, A.; Titerence, R.; Bunnell, S. C.; Barr, V. A.; Samelson, L. E. Dynamic Molecular Interactions Linking the T Cell Antigen Receptor to the Actin Cytoskeleton. *Nat. Immunol.* **2005**, *6* (1), 80–89.
- (54) Grakoui, A.; Bromley, S. K.; Sumen, C.; Davis, M. M.; Shaw, A. S.; Allen, P. M.; Dustin, M. L. The Immunological Synapse: A Molecular Machine Controlling T Cell Activation. *Science* **1999**, *285*, 221.
- (55) Cheng, J.; Montecalvo, A.; Kane, L. P. Regulation of NF- $\kappa$ B Induction by TCR/CD28. *Immunol. Res.* **2011**, *50* (2–3), 113–117.
- (56) Aktas, E.; Kucuksezer, U. C.; Bilgic, S.; Erten, G.; Deniz, G. Relationship between CD107a Expression and Cytotoxic Activity. *Cell. Immunol.* **2009**, *254* (2), 149–154.
- (57) Sharpe, A. H.; Freeman, G. J. The B7-CD28 Superfamily. *Nat. Rev. Immunol.* **2002**, *2* (2), 116–126.
- (58) Alegre, M. L.; Frauwirth, K. A.; Thompson, C. B. T-Cell Regulation by CD28 and CTLA-4. *Nat. Rev. Immunol.* **2001**, *1* (3), 220–228.
- (59) Acuto, O.; Michel, F. CD28-Mediated Co-Stimulation: A Quantitative Support for TCR Signalling. *Nat. Rev. Immunol.* **2003**, *3* (12), 939–951.
- (60) Zang, X.; Allison, J. P. The B7 Family and Cancer Therapy: Costimulation and Coinhibition. *Clin. Cancer Res.* **2007**, *13* (18), 5271–5279.
- (61) Wang, B.; Maile, R.; Greenwood, R.; Collins, E. J.; Frelinger, J. A. Naive CD8 + T Cells Do Not Require Costimulation for Proliferation and Differentiation into Cytotoxic Effector Cells. *J. Immunol.* **2000**, *164* (3), 1216–1222.
- (62) Mossman, K. D.; Campi, G.; Groves, J. T.; Dustin, M. L. Immunology: Altered TCR Signaling from Geometrically Repatterned Immunological Synapses. *Science* **2005**, *310* (5751), 1191–1193.
- (63) Manz, B. N.; Jackson, B. L.; Pettit, R. S.; Dustin, M. L.; Groves, J. T. Cell Triggering Thresholds Are Modulated by the Number of Antigen within Individual T-Cell Receptor Clusters. *Proc. Natl. Acad. Sci. U. S. A.* **2011**, *108* (22), 9089–9094.
- (64) Doh, J.; Irvine, D. J. Immunological Synapse Arrays: Patterned Protein Surfaces That Modulate Immunological Synapse Structure Formation in T Cells. *Proc. Natl. Acad. Sci. U. S. A.* **2006**, *103*, 5700–5705.
- (65) O'Connor, R. S.; Hao, X.; Shen, K.; Bashour, K.; Akimova, T.; Hancock, W. W.; Kam, L. C.; Milone, M. C. Substrate Rigidity Regulates Human T Cell Activation and Proliferation. *J. Immunol.* **2012**, *189* (3), 1330–1339.
- (66) Mordechay, L.; Le Saux, G.; Edri, A.; Hadad, U.; Porgador, A.; Schwartzman, M. Mechanical Regulation of the Cytotoxic Activity of Natural Killer Cells. *ACS Biomater. Sci. Eng.* **2021**, *7* (1), 122–132.
- (67) Liu, B.; Chen, W.; Evavold, B. D.; Zhu, C. Accumulation of Dynamic Catch Bonds between TCR and Agonist Peptide-MHC Triggers T Cell Signaling. *Cell* **2014**, *157* (2), 357–368.